DALTON

Kinetics and mechanism of the cobaloxime(II)-catalysed oxidation of 2-aminophenol by dioxygen. A phenoxazinone synthase model involving free-radical intermediates

László I. Simándi,* Teréz Barna and Sándor Németh

Central Research Institute for Chemistry, Hungarian Academy of Sciences, H-1525 Budapest, PO Box 17, Hungary

Cobaloxime(II) derivatives catalysed the oxidative dehydrogenation of 2-aminophenol (ap) to 2-amino-3*H*-phenoxazin-3-one by dioxygen under ambient conditions. The 2-aminophenoxyl radical (ap$^{\bullet}$) and a cobalt-bound dimeric radical have been detected as intermediates. The kinetics was followed by monitoring dioxygen uptake. The cobaloxime(II) concentration is very low during the reaction as evidenced by ESR spectroscopy. According to the proposed mechanism, in the rate-determining step superoxocobaloxime abstracts an H atom from ap *via* a hydrogen-bonded intermediate, affording the ap$^{\bullet}$ radical. In the steady state cobaloxime(III) predominates and the active catalyst is generated in low concentration *via* its reduction by the ap$^{\bullet}$ radical. The system studied serves as a model of phenoxazinone synthase and calls attention to the possible involvement of radical intermediates in the enzymatic reaction.

Recently there has been a surge of interest in the role of free radicals in metalloenzymes,[1] specific examples being tyrosyl radicals in galactose oxidase[2-4] and ribonucleotide reductase.[5] The involvement of free-radical pathways in enzyme-mediated redox reactions receives increasing attention. In contrast to views persisting until recently about the deleterious (toxic, mutagenic) roles of free radicals, it is now recognized that they often perform key functions essential to the operation of metalloenzymes. These expanding developments have created the new field of free-radical enzymology. One can anticipate that the modelling of such enzymes will attract increasing attention in the future.

The catalytic activation of dioxygen by transition-metal complexes has been extensively studied,[6] one of the main objectives being elucidation of the reaction mechanisms *via* modelling of oxygenases, dehydrogenases and related metalloenzymes. Important groups of substrates used in these studies have been phenol and catechol derivatives, which provide valuable mechanistic information and are sometimes also of synthetic utility.

In the present paper we report studies on a phenoxazinone synthase model system, which uses dioxygen and involves free radicals as key intermediates, being thereby relevant to both the above aspects of metalloenzyme action.

Actinomycin D[7,8] **2**, a naturally occurring antineoplastic agent, is used clinically for the treatment of certain types of cancer.[9] In the last stage of its biosynthesis the 2-aminophenol derivative **1** is catalytically converted into **2** in the presence of dioxygen and phenoxazinone synthase,[8,10] a type 2 copper-containing oxidase isolated from *Streptomyces* (subunit molecular mass 88 000, 3.7 Cu per subunit),[11] Scheme 1. The mechanism of this six-electron oxidative-coupling process has been studied using 2-aminophenols as substrates.[11] It has been suggested that the reaction takes place *via* a sequence of three consecutive two-electron oxidations, alternating with conjugate addition of the 2-aminophenol moiety to *o*-benzoquinone imine type intermediates, followed by tautomerization steps.[11]

Actinomycin biosynthesis has generated interest in the conversion of 2-aminophenol into 2-amino-3*H*-phenoxazine-3-one catalysed by transition-metal complexes, with a view to the possible modelling of phenoxazinone synthase activity. 2-Aminophenol, an analogue of catechol, has also been found to

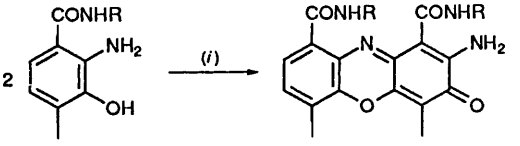

1 2

Scheme 1 R = Cyclic pentapeptide. (*i*) Phenoxazinone synthase, O_2

be a substrate of tyrosinase, which, due to its catecholase activity, converts it first into *o*-benzoquinone monoimine and subsequently into questiomycin.[12] This points to a logical connection between the modelling of both enzymes.

Although replacement of copper by cobalt in tyrosinase leads to the loss of activity,[13] macrocyclic cobalt(II) complexes catalyse the oxidative dehydrogenation of 2-aminophenol in the same way as does the enzyme. However, these cobalt complexes also reveal the additional feature of a remarkable phenoxazinone synthase activity. We have found that 2-aminophenol can be catalytically oxidized to 2-aminophenoxazin-3-one with O_2 in the presence of cobalt(II) salts,[14] a cobalt(II) phthalocyanine[15] derivative, and some cobaloxime(II) derivatives.[16] Stoichiometric oxidation with $K_3Fe(CN)_6$ also affords 2-aminophenoxazin-3-one *via* *o*-benzoquinone imine as intermediate.[17] The complex [Co(salen)] [H_2salen = *N*,*N*′-bis(salicylidene)-ethane-1,2-diamine] as catalyst mediates the conversion of 2-aminophenol into 2,2′-dihydroxyazobenzene.[18]

We have recently reported that, in the presence of cobaloxime(II) derivatives as catalysts for 2-aminophenol oxidation, two free-radical species can be identified by ESR spectroscopy as reaction intermediates.[16] One is the 2-aminophenoxyl radical, observed at early stages of the reaction, demonstrating that *o*-benzoquinone monoimine is formed in two successive one-equivalent steps. We have also established that the ESR spectrum of cobaloxime(II) does not appear during the reaction, indicating that the catalyst is present in an ESR-inactive form. Significantly, the spectrum of the μ-peroxo-dicobaloxime, known to form upon oxygenation of [Co(Hdmg)$_2$L] (H_2dmg = dimethylglyoxime) derivatives in the absence of substrates, is not observed during oxidation of 2-aminophenol.

In view of these features, it was of interest to carry out a kinetic study of the cobaloxime(II)-catalysed oxidation of

Table 1 Dioxygen absorption and concentrations of ap and apx in the reacting mixture[a]

t/min	O_2 absorbed/mmol	[ap]/mmol dm^{-3}	[apx]/mmol dm^{-3}	N_{apx}[b]	N_{ap}[c]
0.0	0.00	25.0	0.00	0.00	0.00
7.0	0.22	20.0	1.81	1.04	0.37
16.0	0.46	17.0	2.82	1.35	0.47
27.0	0.67	13.3	3.90	1.45	0.48
41.0	0.91	11.0	5.10	1.51	0.54
58.0	1.20	9.0	6.25	1.49	0.58
82.0	1.34	5.4	7.25	1.54	0.57
127.0	1.56	3.0	8.63	1.50	0.59
242.0	1.74	2.1	9.56	1.51	0.63
24 h	1.89	1.7	10.4	1.52	0.67
Required by Scheme 2		0.0	12.5	1.50	0.75

[a] $[ap]_0 = 25.0$ mmol dm^{-3}, $[Co(Hdmg)_2(AsPh_3)_2]_0 = 2.5$ mmol dm^{-3}; solvent MeOH (120 cm^3); $T = 303$ K; $P_{O_2} = 7.9 \times 10^4$ Pa. [b] N_{apx} is the amount of O_2 absorbed (mol) for 1 mol of apx formed. [c] N_{ap} is the amount of O_2 absorbed (mol) for 1 mol of ap consumed.

2-aminophenol by dioxygen, with the objective of establishing a reaction mechanism which accommodates the known facts.

Experimental

Analytical grade chemicals were used throughout. Cobaloxime complexes were synthesized by known procedures or slight modifications thereof.[19] 2-Aminophenol (Reanal, Hungary) was recrystallized from Pr^{i}OH (m.p. 177 °C). 2-Aminophenoxazin-3-one (m.p. 254–256 °C) was also prepared by oxidation of 2-aminophenol with HgO.[20]

The HPLC analyses were made on a Waters 410 instrument with a 991 diode-Array spectrophotometric detector [column, Nucleosil C-18, 5 μm, 250 × 4.6 mm; eluant, 35% acetonitrile–65% 1 mmol dm^{-3} KH_2PO_4 (pH 3.3) or 80% acetonitrile–20% 1 mmol dm^{-3} KH_2PO_4 (pH 3.3)]. The UV/VIS spectra were recorded on a Hewlett-Packard 8452A diode-array spectrophotometer.

Kinetic measurements were carried out by gas volumetry at atmospheric pressure, at constant partial pressure of O_2, with vigorous stirring. Volume readings were taken at about 1 min intervals by timing the equalization of about 1 mm differences in the mercury levels. The shapes of dioxygen absorption curves were independent of the stirring rate, which excludes the influence of mass transport.

The ESR spectra were recorded on a JES-ME-3X instrument.

Results and Discussion

Products of 2-aminophenol oxidation

We have found that the oxidation of 2-aminophenol to 2-aminophenoxazin-3-one by O_2 is catalysed by the cobaloxime(II) derivatives $[Co(Hdmg)_2L_2]$ (L = PPh_3, $AsPh_3$ or $SbPh_3$) (Scheme 2). The reaction takes place at room temperature and 1 bar (10^5 Pa) O_2 pressure in MeOH or acetone as solvents. We monitored this reaction by measuring the volume of dioxygen absorbed by the solution and simultaneously the amount of 2-aminophenol, 2-aminophenoxazin-3-one and any other component by HPLC. Samples withdrawn from the reaction mixture were diluted 10-fold by the eluant to stop the reaction before injection. The ESR spectra of the reacting mixture were recorded after freezing the solution. The results of a typical run are listed in Table 1.

According to Table 1, no oxidation of the axial ligand $AsPh_3$ is detected. However, upon addition of H_2O_2 to the mixture in increasing amounts up to the quantity that could be expected from the amount of absorbed dioxygen, $AsPh_3O$ is formed in up to 90% yield within 1 h. This is evidence that H_2O_2 is *not* an intermediate of 2-aminophenol oxidation.

It can also be established from Table 1 that at the end of the run the number of moles of O_2 used for each mol of

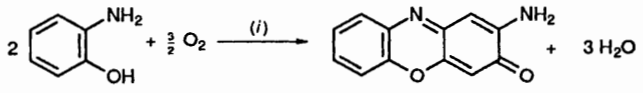

Scheme 2 (*i*) $[Co(Hdmg)_2L_2]$, MeOH

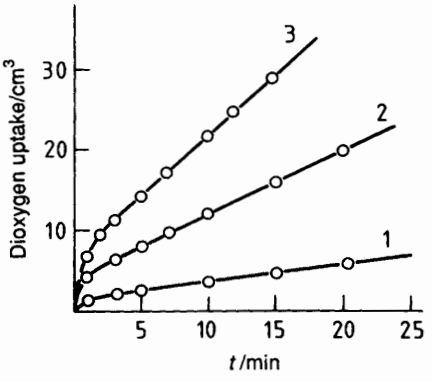

Fig. 1 Typical dioxygen uptake curves for the catalytic oxidation of 2-aminophenol. $[Co]_0 = 1.0 \times 10^{-3}$ (1), 2.5×10^{-3} (2) or 5.0×10^{-3} (3), $[ap]_0 = 5.0 \times 10^{-2}$ and $[O_2] = 1.1 \times 10^{-3}$ mol dm^{-3}; $T = 303$ K; solvent MeOH

2-aminophenoxazin-3-one (apx) produced (N_{apx}) is 1.50 ± 0.02, indicating the validity of the overall stoichiometry given by Scheme 2. However, this would also require $N_{ap} = 0.75$ mol O_2 per mol 2-aminophenol (ap) consumed, but only 0.67 mol per mol was found by HPLC on combination with gas volumetry. Consequently, the missing phenol (*ca.* 5–10 mol%) is tied up in reaction intermediates without having been oxidized (*i.e.* without having consumed O_2). The amount of such intermediates is greater in the initial stages of the reaction, as indicated by the values of N_{apx} (*ca.* 1.0) and N_{ap} (*ca.* 0.4).

Stoichiometry of dioxygen uptake

Volumetric dioxygen absorption curves have been recorded at various reactant concentrations and dioxygen pressures. Typical curves are shown in Fig. 1 for increasing cobaloxime concentration. The uptake is initially rapid until about 0.6 mol O_2 per mol Co has been consumed, then the rate decreases to a steady-state value, which persists for extended periods of time, permitting facile evaluation. Fig. 2 displays the amount of O_2 absorbed in the rapid stage, as determined by extrapolation of the linear section to zero time, as a function of the initial cobaloxime concentration. The slope of the straight line obtained is 0.58 ± 0.03, indicating a mixture of 1 : 1 and 1 : 2 O_2 to cobaloxime stoichiometries. A 1 : 1 stoichiometry corresponds to the known superoxocobaloxime(III), $[Co(Hdmg)_2L(O_2)]$ and/or $[Co(Hdmg)_2L(O_2H)]$ formed *via* H-atom abstraction from the substrate. A 1 : 2 stoichiometry can in principle be

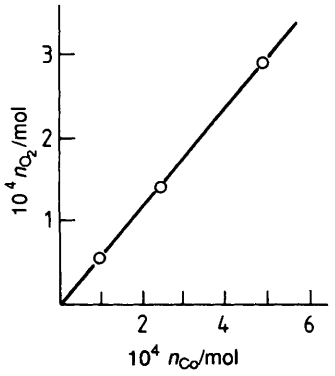

Fig. 2 Amount of O_2 absorbed in the rapid initial phase as a function of the amount of cobaloxime(II) added (from the linear sections of the curves in Fig. 1 extrapolated to zero time)

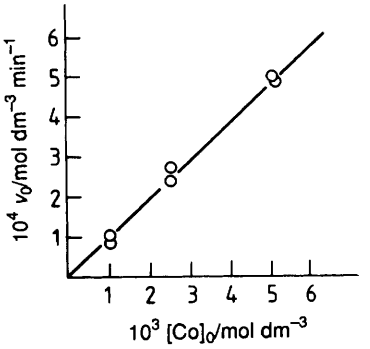

Fig. 3 Dependence of rate of dioxygen absorption (v_0) on the catalyst concentration in the steady state after the rapid initial phase. $[ap]_0$ = 5.0×10^{-2}, $[O_2] = 1.1 \times 10^{-3}$ mol dm^{-3}; T = 303 K; solvent MeOH

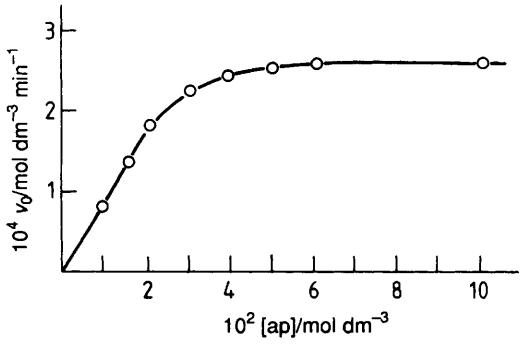

Fig. 4 Dependence of the rate of dioxygen absorption (v_0) on the substrate (ap) concentration in the steady state after the rapid initial phase. $[Co]_0 = 2.5 \times 10^{-3}$, $[O_2] = 1.1 \times 10^{-3}$ mol dm^{-3}; T = 303 K; solvent MeOH

accounted for by formation of μ-peroxo-dicobalt complexes of the type Co–O–O–Co, where Co represents the cobaloxime moiety. However, UV/VIS spectra show that very little, if any, μ-peroxo species is present during the reaction. Thus a different interpretation of the 1:2 stoichiometry is required. As no ESR signal due to cobaloxime(II) or superoxocobaloxime(III) species was detected in the system, we propose that the predominant fraction of the starting cobaloxime(II) is co-oxidized with 2-aminophenol to hydroxocobaloxime(III) in the rapid first section, as given by the overall equation (1). This equation is

$$Co^{II} + O_2 + ap \longrightarrow Co^{III}(OH) + ap^{\bullet} + \tfrac{1}{2}O_2 \quad (1)$$

written to indicate that the corresponding stoichiometry of 1:2 is the result of dioxygen uptake and release steps, rather than that of a single reaction. The mechanism of this process will be discussed later.

Kinetic measurements

The volumetric dioxygen absorption curves recorded at various reactant concentrations and dioxygen pressures have been used for determination of the kinetics. The kinetic analysis was based on the uptake rates (v_0) measured *after* the rapid initial section, on the linear part of the curve, when the catalytic system has reached a steady state. Thus a first-order dependence of the steady-state rate v_0 on the total cobaloxime(II) concentration, $[Co]_0$ (Fig. 3), was found. The absorption rate increases with substrate concentration, $[ap]_0$ (Fig. 4), and dioxygen pressure (Fig. 5), limiting rates being reached in both cases.

Upon plotting the data as reciprocal steady-state rates (v_0^{-1}) from Figs. 4 and 5 against the reciprocal of the concentrations of ap and O_2 excellent linear dependences are obtained (Figs. 6 and 7), demonstrating that the observed kinetic behaviour is consistent with the proposed reaction mechanism (see below).

Reaction mechanism

The observed kinetic behaviour in combination with the non-kinetic information available permits the derivation of a reaction mechanism consistent with all the results summarized in the previous sections. A suitable mechanism should: (1) be in agreement with the observed kinetics; (2) provide a path for regeneration of the cobaloxime(II) catalyst at the end of the cycle; (3) incorporate the 2-aminophenoxyl radical as an intermediate, because this species has been detected by ESR spectroscopy during the reaction. It should also explain: (4) how the dioxygen molecule enters the cycle and how it is transformed to the observed product of its reduction (H_2O rather than H_2O_2); (5) why the paramagnetic cobaloxime(II) or the superoxocobaloxime, $Co^{III}(O_2^{\bullet -})$, species are not present at ESR-detectable levels during the reaction, and what is the predominant form of the added cobaloxime in the steady state; (6) the observed stoichiometry of O_2:Co = 1:2 at the end of the rapid initial section without invoking the μ-peroxo-dicobaloxime species (its absence is proved by the lack of its characteristic UV/VIS spectrum).

We propose that equations (2)–(7) describe the observed

$$Co^{II} + O_2 \underset{}{\overset{K_1}{\rightleftharpoons}} Co^{III} + O_2 \quad (2)$$

$$Co^{III}(O_2) + ap \overset{K_2}{\rightleftharpoons} \mathbf{X} \quad (3)$$

$$\mathbf{X} \xrightarrow{k_3} Co^{III}(O_2H) + ap^{\bullet} \quad (4)$$

$$2\,Co^{III}(O_2H) \xrightarrow[k_4]{\text{fast disprop.}} 2\,Co^{III}(OH) + O_2 \quad (5)$$

(equivalent to: $2\,HO_2^- \longrightarrow 2\,HO^- + O_2$)

$$Co^{III}(OH) + ap^{\bullet} \xrightarrow{\text{fast } (k_5)} bqmi + Co^{II} + H_2O \quad (6)$$

$$2\,ap^{\bullet} \xrightarrow{\text{fast } (k_6)} bqmi + ap \quad (7)$$

behaviour of the system up to the formation of the key intermediate *o*-benzoquinone monoimine (bqmi). Its further conversion into the product apx can be rationalized by the reactions described in ref. 16. Here Co^{II} represents $Co(Hdmg)_2$ and $ap^{\bullet}$ is the 2-aminophenoxyl radical.

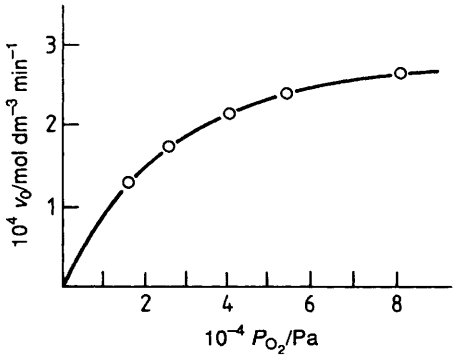

Fig. 5 Dependence of rate of dioxygen absorption (v_0) on the dioxygen partial pressure in the steady state after the rapid initial phase. $[Co]_0 = 2.5 \times 10^{-3}$, $[ap]_0 = 3.0 \times 10^{-2}$ mol dm^{-3}; $T = 303$ K; solvent MeOH

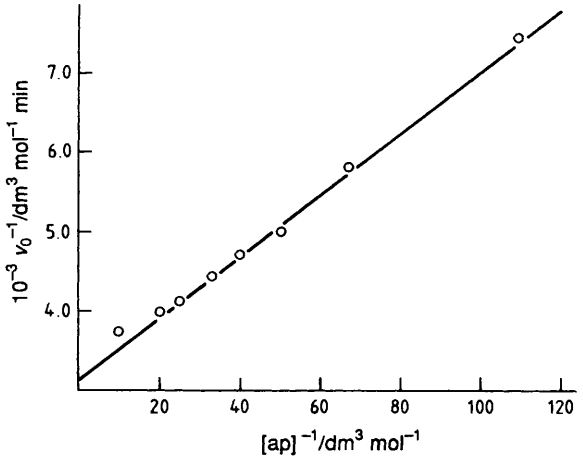

Fig. 6 Dependence of $(v_0)^{-1}$ on $[ap]^{-1}$. Conditions as in Fig. 4

In this mechanism the active catalyst is formed *via* the loss of the axial ligands from $[Co(Hdmg)_2(AsPh_3)_2]$ upon dissolution in MeOH, then a superoxocobaloxime derivative is formed in a rapid pre-equilibrium (2). The substrate ap is hydrogen bonded *via* its OH group to the external superoxo oxygen in a subsequent rapid equilibrium (3). Intramolecular H-atom transfer in the hydrogen-bonded complex **X** is the rate-determining step, generating the *o*-aminophenoxyl radical in (4). Reaction (5), leading to regeneration of $\frac{1}{2}O_2$, serves to explain two important facts. One is that the volumetric dioxygen absorption curves exhibit a sharp break after the uptake of about 0.5 mol O_2 per mol Co, but, as shown by UV/VIS spectra, at that moment the solution contains only traces of the μ-peroxo-dicobaloxime(III), which would correspond to that stoichiometry. The other fact is that, according to ESR measurements, neither the paramagnetic cobaloxime(II) nor the superoxocobaloxime, $Co^{III}(O_2^{\bullet -})$,[19] can be detected in the reacting system.

Reaction (6), *i.e.* the reduction of the catalytically inactive hydroxocobaloxime(III) by the free aminophenoxyl radical, represents the major new feature of this mechanism as the path of catalyst regeneration. Disproportionation (7) is a channel for removal of the surplus ap$^{\bullet}$ from the system.

Thus during the catalytic reaction (Scheme 2) cobalt is predominantly present as the hydroxocobaloxime(III), Co^{III}-(OH), which by itself does not react with ap, as demonstrated by experiments under N_2. However, the autocatalytic oxidation of ap can be observed under O_2 in the presence of a known precursor[19] of $Co^{III}(OH)$ (Fig. 8). This is apparently due to the slow autoxidation of ap starting with step (8), followed by (2)–(7). The net result is dioxygen absorption, product formation (bqmi), as well as generation of the active catalyst Co^{II} and

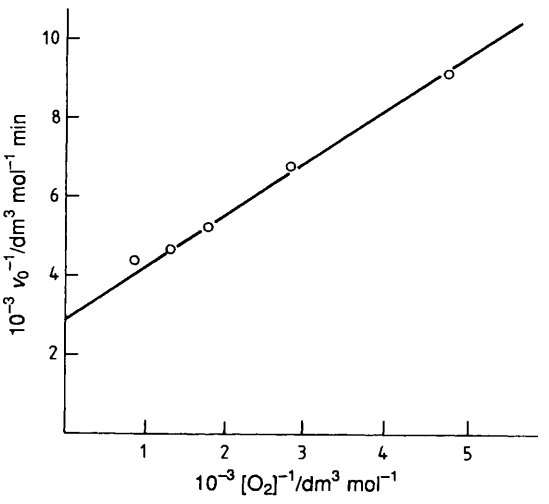

Fig. 7 Dependence of $(v_0)^{-1}$ on $[O_2]^{-1}$. Conditions as in Fig. 5

free radical ap$^{\bullet}$, capable of effecting further ap oxidation [equation (9)]. This process occurs with increasing rate, leading to a sigmoidal dioxygen absorption curve. Following this the cobaloxime(II) formed will catalyse the reaction as shown by equations (2)–(7). This catalytic cycle is accessible to kinetic studies only up to the formation of bqmi.

$$ap + O_2 \longrightarrow ap^{\bullet} + HO_2 \quad (8)$$

$$Co^{III}(OH) + ap^{\bullet} \longrightarrow Co^{II} + bqmi + H_2O \quad (6)$$

$$Co^{II} + O_2 + ap \rightarrowtail\!\!\!\!\rightarrow Co^{III}(OH) + ap^{\bullet} + \tfrac{1}{2}O_2 \quad (2)\text{–}(5)$$

$$2\,ap + \tfrac{1}{2}O_2 + Co^{III}(OH) \longrightarrow bqmi + ap^{\bullet} + H_2O + Co^{II} \quad (9)$$

The rate equation corresponding to this mechanism can be derived on the assumption that steps (2) and (3) are pre-equilibria and (4) is rate determining. The mass balance for cobaloxime species at the low conversions where the steady-state rates were determined is given by equation (10), neglecting

$$[Co]_0 = [Co^{II}] + [Co^{III}O_2] + [\mathbf{X}] + [Co^{III}(OH)] \quad (10)$$

the concentrations of the Co–O–O–Co type μ-peroxo-dicobaloxime(III) and the hydroperoxocobaloxime(III), $Co^{III}(O_2H)$. This is justified by the failure to observe the known UV/VIS spectrum of the μ-peroxo species, and by the rapidity of disproportionation step (5). The absence of cobalt(II)-type ESR signals throughout the reaction points to the rather low concentration of Co^{II}. These species are important kinetically as they ensure the activation of O_2, however they can be neglected in the mass-balance equation (10).

By combining equation (10) with the expressions for the equilibrium constants of reactions (2) and (3), we can express the concentration of **X**, which in turn can be used to derive rate equation (11) (assuming that $K_2[ap]_0 \gg 1$).

$$v_0 = k_3[\mathbf{X}] = k_3 \frac{\{[Co]_0 - [Co^{III}(OH)]\}K_1K_2[Co]_0[ap]_0[O_2]}{1 + K_1K_2[ap]_0[O_2]} \quad (11)$$

On grounds of the observed behaviour, we propose that the predominant part of the total cobaloxime is present as the complex $Co^{III}(OH)$, which reaches an approximately constant, steady-state concentration during the rapid initial stage of the reaction. In order to evaluate the kinetic data, we need an expression for this concentration to be used in equation (11) describing the kinetic behaviour in the subsequent linear

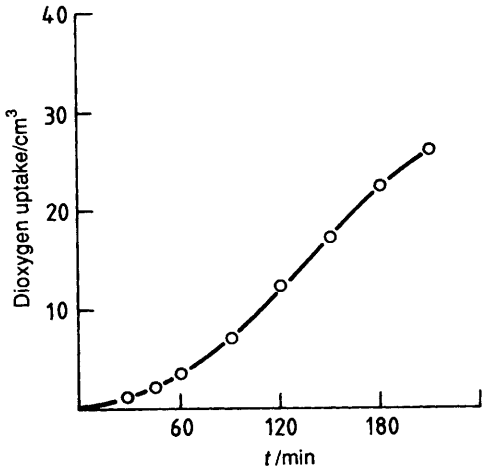

Fig. 8 Autocatalytic absorption of O_2 in the presence of cobaloxime(III). $[Co(Hdmg)_2(py)Cl]_0 = 5.0 \times 10^{-3}$, $[ap]_0 = 5.0 \times 10^{-2}$, $[O_2] = 1.1 \times 10^{-3}$ mol dm^{-3}; $T = 303$ K; solvent MeOH (100 cm^3). py = Pyridine

dioxygen-uptake section. This can be obtained from the following considerations. According to Fig. 2 the amount of O_2 (n in mol dm^{-3} units) absorbed in the rapid section in excess of the solubility is $0.57[Co]_0$. This amount corresponds to the sum of species related to the dioxygen concentration and can be written as in equation (12). The factor of 0.57 is the average

$$n = [CoO_2] + [\mathbf{X}] + 0.5[Co^{III}(OH)] = 0.57[Co]_0 \quad (12)$$

amount of O_2 (mol) absorbed per mol of cobaloxime in the initial stage of the reaction, where the kinetic measurements were carried out.

Combination of equations (10) and (12) provides the approximate expression (13) for the steady-state concentration

$$[Co^{III}(OH)] \approx 0.86[Co]_0 \quad (13)$$

of $Co^{III}(OH)$. Thus the kinetic equation (11) can be rewritten as in (14). The experimental results in Figs. 3–7 are readily

$$v_0 = k_3 \frac{0.14K_1K_2[Co]_0[ap]_0[O_2]}{1 + K_1K_2[ap]_0[O_2]} \quad (14)$$

accommodated by rate law (14), demonstrating consistency of the observed kinetic behaviour with the mechanism in equations (2)–(7). The rate and equilibrium constants have been determined from the slopes and intercepts of the excellent linear plots of $(v_0)^{-1}$ *vs.* $[ap]^{-1}$ (Fig. 6) and $(v_0)^{-1}$ *vs.* $[O_2]^{-1}$ (Fig. 7) and are listed in Table 2. The experimental slopes of the plots of $(v_0)^{-1}$ *vs.* $[O_2]^{-1}$ and v_0 *vs.* $[Co]_0$ plots (1.34 min and 0.096 min^{-1}, respectively) are in good agreement with the values calculated from equation (14) (1.54 min and 0.10 min^{-1}, respectively) using the constants in Table 2.

An important assumption was made in deriving rate equation (14) from the proposed mechanism, which is expressed by equation (13). This is that in the rapid initial section most of the added cobaloxime(II) is converted into $Co^{III}(OH)$, the concentration of which remains practically constant for long periods of time, producing steady-state dioxygen-uptake rates (v_0). The fraction of $Co^{III}(OH)$ can be estimated as *ca.* 86% by extrapolating v_0 to $t = 0$. The validity of this assumption can be demonstrated by simulating the behaviour of the system *via* numerical integration based on the mechanism. The experimentally determined rate and equilibrium constants given in Table 2 were retained and the rest of the constants needed were adjusted so as to achieve the best fit of the measured and calculated dioxygen-uptake curves. Earlier data for the required constants ($K_1 = k_1/k_{-1}$ and $K_2 = k_2/k_{-2}$) were used as starting points for the estimated values.[21,22] The best fit was found for the set of constants listed in Table 3.

Typical experimental and simulated dioxygen-absorption *vs.* time curves are shown in Fig. 9, together with the simulated $[Co^{III}(OH)]$ *vs.* time curve for the given experiment. Clearly, the near-constancy of $[Co^{III}(OH)]$ is inherent in the model used and is fulfilled starting from about 220 s within approximately 10%. From 400 s, when the apx conversion is about 20%, the approximation becomes better than ± 5%, *i.e.* it is quite good throughout most of the catalytic process.

It should be noted that some of the steps involved in the mechanism have their analogues in the catalytic oxidation of hindered phenols by O_2 in the presence of various cobalt(II) salen-type complexes.[6a] Thus Nishinaga *et al.*[23] included step (2), followed by the sum of (3) and (4), as well as (5), into their six-step mechanism for the stoichiometric formation of peroxoquinolinolatocobalt(III) complexes. In work on the catalytic oxidative coupling of 2,6-disubstituted phenols, Drago and co-workers[24,25] proposed the type of hydrogen-bonding interaction represented by step (3). Gaudemer and co-workers[26] pointed out the role of water in similar reactions in organic solvents.

The key new feature of our mechanism is step (6), which has not been considered before. It provides a way to explain how catalytic dioxygen activation can occur *via* cobaloxime(II), with hydroxocobaloxime(III) being the predominant cobalt species during the reaction.

The overall reaction (Scheme 2) requires several further addition and oxidative dehydrogenation steps involving ap, O_2 and bqmi as reactants on the way to apx. The numerical integration procedure used to simulate the behaviour of the catalytic system required the formal reaction (15), because some

$$ap + bqmi + O_2 \xrightarrow[-2H_2O]{k_{apx}} apx \quad (15)$$

apx can be detected shortly after the start of the reaction. The mechanism of the overall transformation (15) is obviously complex. Earlier, we had identified two free-radical intermediates in our system, *viz.* 2-aminophenoxyl and another which may have the structure **I**.[16] Alternatively, its ESR data[16] are consistent also with structure **II**, which may be formed *via* the hydration of (bqmi)Co^{II} followed by one-electron oxidation. However, if formed, **II** should be a by-product, because the corresponding *p*-benzoquinone cannot be converted into apx, as demonstrated by Barry *et al.*[11] On the other hand, **I** is a detectable isomeric radical of the very reactive intermediate leading to apx.[16]

The mechanism emerging from our kinetic study represents a model for phenoxazinone synthase and a possible model for the diphenolase activity of tyrosinase. It is remarkable that the overall dehydrogenation to bqmi involves a 2-aminophenoxyl free radical as intermediate, which is also the key species ensuring regeneration of the active cobaloxime(II) catalyst.

Recent studies on the copper-containing enzyme phenoxazinone synthase have been aimed at elucidating the mechanism of transformation of ap to apx,[10,11] considering earlier suggestions.[27] In that research intermediates of the enzymatic reaction have been isolated and synthesized by independent routes to observe their behaviour upon exposure to the enzyme. The sequence of stable intermediates has been established but no free radicals have been detected in the enzymatic reaction. The present results indicate that the system may merit reconsideration.

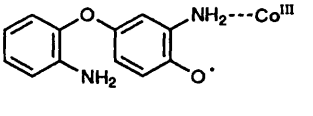

I

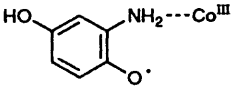

II

Table 2 Rate and equilibrium constants determined from kinetic law (14). *

Constant	Value	Source
k_3	$(1.56 \pm 0.07) \times 10^{-2}$ s^{-1}	Intercepts of $(v_0)^{-1}$ *vs.* $[O_2]^{-1}$ and *vs.* $[ap]^{-1}$
K_1K_2	$(7.2 \pm 0.35) \times 10^4$ dm^6 mol^{-2}	Slopes of $(v_0)^{-1}$ *vs.* $[O_2]^{-1}$ and *vs.* $[ap]^{-1}$

* T = 303 K, solvent methanol.

Table 3 Rate and equilibrium constants giving the best fit of simulated and calculated dioxygen-uptake curves

$k_1 = 9.0 \times 10^{-3}$ dm^3 mol^{-1} s^{-1} $k_{-1} = 6.61 \times 10^{-4}$ s^{-1} $k_2 = 1.32 \times 10^2$ dm^3 mol^{-1} s^{-1} $k_{-2} = 2.5 \times 10^{-2}$ s^{-1}	$K_1K_2 = 7.2 \times 10^4$ M^{-2} (exptl.)
$k_3 = 1.56 \times 10^{-2}$ s^{-1} (exptl.)	$k_4 = 20$ dm^3 mol^{-1} s^{-1}
$k_5 = 50$ dm^3 mol^{-1} s^{-1}	$k_6 = 1.0 \times 10^3$ dm^3 mol^{-1} s^{-1}
$k_{apx} = 3.0 \times 10^{-2}$ dm^3 mol^{-1} s^{-1}	[formal reaction (15) accounting for apx formation]

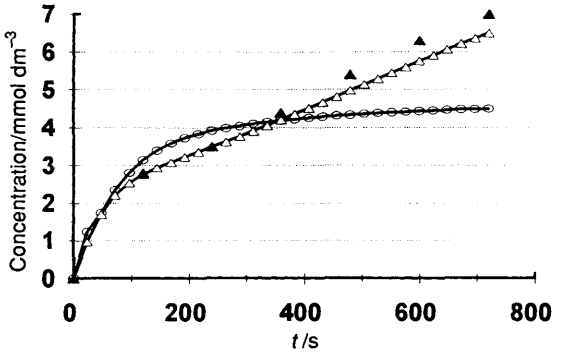

Fig. 9 Experimental (▲) and simulated (△) dioxygen-absorption curves and the $[Co^{III}(OH)]$ *vs.* time curve (○) from numerical integration based on the set of constants in Table 3. $[Co]_0 = 5.0 \times 10^{-3}$, $[ap]_0 = 5.0 \times 10^{-2}$, $[O_2] = 1.1 \times 10^{-3}$ mol dm^{-3}; T = 303 K; solvent MeOH

An additional point of importance emerging from this work is the role of free radicals in catalytic cycles not just as reaction intermediates but also as 'cofactors' involved in the regeneration of the catalytic site. In this context the reaction between the deactivated cobaloxime(III), $Co^{III}(OH)$, and the free radical ap$^{\bullet}$ in step (6) of the proposed mechanism may be regarded as a model of active site reproduction. The substrate itself (ap) does not have a sufficiently negative redox potential to react directly with the 'spent' catalyst at acceptable rates. However, the intermediate of substrate oxidation, *viz.* the ap$^{\bullet}$ radical formed upon interaction of dioxygen with cobaloxime(II), is capable of closing the gap in redox potential, thereby ensuring regeneration of the active cobaloxime(II) and sustaining the catalytic cycle with minimum input of energy.

Acknowledgements

This work was supported by the Hungarian Research Fund (OTKA Grant 1776), COST Chemistry Action D1 (PECO grant 12984) and the Phare Accord Programme (H 9112-0108).

References

1 E.-I. Ochiai, in *Metal Ions in Biological Systems*, eds. H. Sigel and A. Sigel, Marcel Dekker, New York, Basel, 1994, vol. 30, pp. 1–24.
2 J. W. Whittaker, *Metal Ions in Biological Systems*, eds. H. Sigel and A. Sigel, Marcel Dekker, New York, Basel, 1994, vol. 30, pp. 315–403.
3 N. Ito, S. E. V. Phillips, C. Stevens, Z. B. Ogel, M. J. McPherson, J. K. Keen, K. D. S. Yadav and P. F. Knowles, *Nature (London)*, 1991, **350**, 87.
4 A. J. Thomson, *Nature (London)*, 1991, **350**, 22.
5 K.-Y. Lam, D. G. Fortier and A. G. Sykes, *J. Chem. Soc., Chem. Commun.*, 1990, 1019.
6 (*a*) L. I. Simándi, *Catalytic Activation of Dioxygen by Metal Complexes*, Kluwer Academic Publishers, Dordrecht, Boston, London, 1992; (*b*) D. H. R. Barton, A. E. Martell and D. T. Sawyer (Editors), *The Activation of Dioxygen and Homogeneous Catalytic Oxidation*, Plenum, New York and London, 1993; (*c*) L. I. Simándi (Editor), *Dioxygen Activation and Homogeneous Catalytic Oxidation; Studies in Surface Science and Catalysis*, Elsevier, Amsterdam, Oxford, New York, Tokyo, 1991, vol. 66.
7 U. Hollstein, *Chem. Rev.*, 1974, **74**, 625.
8 E. Katz and H. Weissbach, *J. Biol. Chem.*, 1962, **237**, 882.
9 E. Frei, *Cancer Chemother. Rep.*, 1974, **58**, 49.
10 C. E. Barry, P. Nayar and T. P. Begley, *J. Am. Chem. Soc.*, 1988, **110**, 3333.
11 C. E. Barry, III, P. G. Nayar and T. P. Begley, *Biochemistry*, 1989, **28**, 6323.
12 O. Toussaint and K. Lerch, *Biochemistry*, 1987, **26**, 8567.
13 K. Lerch, in *Metal Ions in Biological Systems*, ed. H. Sigel, Marcel Dekker, New York and Basel, 1981, vol. 13, pp. 143–186.
14 L. I. Simándi, S. Németh and N. Rumelis, *J. Mol. Catal.*, 1987, **42**, 357.
15 Z. Szeverényi, E. R. Milaeva and L. I. Simándi, in *Dioxygen Activation and Homogeneous Catalytic Oxidation; Studies in Surface Science and Catalysis*, ed. L. I. Simándi, Elsevier, Amsterdam, 1991, vol. 66, p. 171.
16 L. I. Simándi, T. M. Barna, L. Korecz and A. Rockenbauer, *Tetrahedron Lett.*, 1993, **34**, 717.
17 T. Nogami, T. Hishida, M. Yamada, H. Mikawa and Y. Shirota, *Bull. Chem. Soc. Jpn.*, 1975, **48**, 3709.
18 F. Benedini, G. Galliani, M. Nali, B. Rindone and S. Tollari, *J. Chem. Soc., Perkin Trans. 2*, 1985, 1963.
19 G. N. Schrauzer and L. P. Lee, *J. Am. Chem. Soc.*, 1970, **92**, 1551.
20 G. W. K. Cavill, *Tetrahedron*, 1961, **12**, 139.
21 L. I. Simándi, C. R. Savage, Z. A. Schelly and S. Németh, *Inorg. Chem.*, 1982, **21**, 2765.
22 L. I. Simándi, A. Fülep-Poszmik and S. Németh, *J. Mol. Catal.*, 1988, **48**, 265.
23 A. Nishinaga, H. Tomita, K. Nishizawa and T. Matsuura, *J. Chem. Soc., Dalton Trans.*, 1981, 1504.
24 A. Zombeck, R. S. Drago, B. B. Corden and J. H. Gaul, *J. Am. Chem. Soc.*, 1981, **103**, 7580.
25 C. B. Bailey and R. S. Drago, *Coord. Chem. Rev.*, 1987, **79**, 321.
26 Frostin-Rio, D. Pujol, C. Bied-Charreton, M. Perrèe-Fauvet and A. Gaudemer, *J. Chem. Soc., Dalton Trans.*, 1984, 1971.
27 W. Schäfer, *Prog. Org. Chem.*, 1964, **6**, 135.

Received 5th July 1995; *Paper* 5/04354I